Microfluidic Networks for Chemical Patterning of Substrates: Design and Application to Bioassays

ARTICLE *in* JOURNAL OF THE AMERICAN CHEMICAL SOCIETY · JANUARY 1998

Impact Factor: 12.11 · DOI: 10.1021/ja973071f

Microfluidic Networks for Chemical Patterning of Substrates: Design and Application to Bioassays

Emmanuel Delamarche, André Bernard,‡ Heinz Schmid, Alexander Bietsch, Bruno Michel, and Hans Biebuyck*

Contribution from the IBM Research Division, Zurich Research Laboratory, CH-8803 Rüschlikon, Switzerland

Received September 2, 1997. Revised Manuscript Received November 6, 1997

Abstract: This article describes the design, function, and application of simple microfluidic networks as conduits for the patterned delivery of chemical reactants onto a substrate. It demonstrates how such networks, made in an elastomer, allow simultaneous delivery of functionally distinct molecules onto targeted regions of a surface (Delamarche, E. *et al. Science* **1997**, *276*, 779−781). Microfluidic networks generally consume less than microliter quantities of solution and are thus well suited for use when the required reagents are scarce or precious, as often occurs in experiments and technologies that place biochemicals on solid planar substrates. We illustrate some of the particular challenges of doing chemistry inside the narrow confines of capillaries defined by fluidic networks, in addition to the advantages attendant to this approach, in the context of forming patterned arrays of different, and functional, immunoglobulins useful in highly localized biological assays.

Introduction

Chemists are well versed in handling macroscopic quantities of reactive solutions needed to effect the myriad of molecular conversions that characterize the field. The divergent requirements of combinatorial chemistry, advanced screening devices, and a fundamental curiosity about the happenings at interfaces call on us to carry out such transformations at ever smaller scales, sometimes at solid substrates where the environment differs substantially from that of the bulk. What serves as the Erlenmeyer flask when areas only a few microns in breadth constitute the volume?

Several methods exist now for carrying out chemistry confined to well-defined regions on a surface, the most successful among which are undoubtedly lithographies based on beams of light, electrons, or ions.[1] A typical feature of these lithographies is the use of an overlayer, often an organic polymer, or special molecules that are the basis for pattern formation on an underlying substrate. Lithographies based on beams are tremendously useful in certain contexts but suffer some disadvantages when applied to molecular patterning. Several steps are usually required before pattern transfer is complete. Dissolution of the overlayer involves a development step that exposes the entire system to organic solvents, plasmas, or otherwise chemically harsh and potentially contaminating conditions. The use of a physical mask on the substrate causes the unproductive loss of material onto the tops of the overlayer, where it can be difficult or impossible to recover. When special molecules are used, as for light-based attachment schemes, generality of the application is lost, and only highly specialized reactions are possible. Carrying out several different reactions simultaneously with different reagents by conventional lithography is generally very difficult or not possible. The masking and patterning steps for each reaction must thus be iterated, making high integration costly and complicated, particularly where overlay accuracy in defining regions of sequential reactions is needed. Microcontact printing (μCP)[2] is undoubtedly the choice for patterning molecules on reactive substrates. The technique is particularly convenient and simple, requiring no extraordinary apparatus or skill to effect micron-scale placement of molecules with submicron resolution. Where different molecules are needed on the same substrate, stamps used in succession can provide a useful means of transfer, particularly in the case of alkanethiols. The step used to "ink" the stamp is potentially harmful to fragile molecules, however. As above, carrying out simultaneous and different chemical reactions on a substrate is not obvious, although the possibility remains. The range and scope of these reactions is certainly limited and, at the very least, must be carried out under conditions divergent from their equivalents in solution.

A different approach to localizing chemical reactions on surfaces is based on the definition of open networks of conduits in an elastomeric polymer, poly(dimethylsiloxane) (PDMS), Figure 1A, to form microfluidic networks (μFNs).[3,4,5] When applied to a substrate, the structured elastomer seals the surface by its conformal contact and makes linked, closed capillaries that fill with liquid reactants and guide them along these conduits with great fidelity to the pattern defined in the elastomer. Sets of such capillaries can be effectively isolated from each other, allowing independence in their supply of reactants from remote, macroscopic reservoirs, Figure 1B.

This paper examines the use of microfluidics for the attachment of arrays of biomolecules on a solid surface as anticipated next-generation bioassays. Many types of bioassays use molecules either captured or passively deposited on a surface from solution with the general aim of diagnostics.[6] Assays of

* To whom correspondence should be addressed.

‡ Also at Biochemisches Institut der Universität Zürich, Winterthurerstrasse 190, CH-8057 Zürich, Switzerland.

(1) Proceedings of the 40th International Conference on Electron, Ion, and Photon Beam Technology and Nanofabrication *J. Vac. Sci. Technol. A* **1996**, *7*.

(2) Xia, Y.; Tien, J.; Qin, D.; Whitesides, G. M. *Langmuir* **1996**, *12*, 4033−4038.

(3) Kim, E.; Xia, Y.; Whitesides, G. M. *Nature* **1995**, *376*, 581−584.

S0002-7863(97)03071-0 CCC: $15.00
Published on Web 01/09/1998

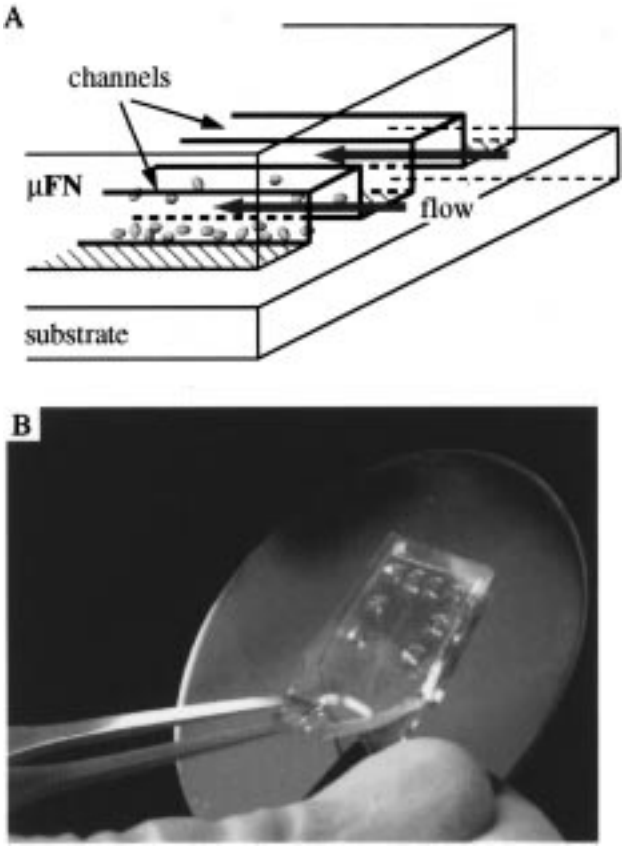

Figure 1. (A) A scheme for a microfluidic network useful for the patterned delivery of reactants to surfaces has a series of predefined openings in a removable overlayer. Its placement on a substrate selectively seals the surface and creates channels of fluid flow between the two. (B) One realization of such a μFN uses a flexible, patterned elastomer, PDMS, having surface reliefs formed by molding the polymer on a lithographically defined master. Adhesion between the elastomer and substrate, a silicon wafer in the case shown here, is sufficient to ensure a highly directed flow of liquids along the surface while remaining sufficiently weak to allow easy removal of the elastomer from the substrate after use. Eight pads, each $\approx$8 mm^3, visible in the upper part of the elastomer provide separate openings for filling selected parts of the network using capillary forces to draw in liquid.

the future will clearly follow the trend toward increased integration, greater sensitivity, higher specificity, and better reliability, ideally while becoming more conservative of reagents. Techniques that allow the patterning of biomolecules by chemical reaction on small regions of a surface should help further these goals.[7−14] First we focus on the rules of fabricating μFNs: What design promotes the stability of its channels when formed in PDMS and their filling by liquid reactants? Next, we demonstrate the consequences of flow through μFNs for the depletion of chemicals available for reaction at remote points in the capillaries where only hydrodynamic forces effect a filling of the network. Finally, we show patterns of immobilized immunoglobulins on various substrates at scales down to 2 μm and illustrate how useful the μFN concept is for the preparation of substrates for miniaturized and simultaneous bioassays.

Experimental Section

Materials and Substrates. All chemicals were of a reagent grade or better and were used as received unless indicated otherwise. Deionized water, produced with a Milli Q Millipore purification unit (Millipore), had a resistivity of $\approx$18.2 Ω cm^{-1}. Lyophilized, polyclonal immunoglobulin G (IgGs) from chicken (Sigma) were reconstituted in phosphate-buffered saline (PBS, pH 7.4) to a concentration of 1 mg mL^{-1}. Monoclonal mouse IgGs (clone X7B3, Department of Biochemistry, University of Zurich) were used as a 0.84 mg mL^{-1} solution in PBS.

Preparation of Substrates for Immobilization of IgGs. Hydrophobic silicon surfaces were obtained by dissolving the native oxide from silicon wafers (10−25 Ω cm^{-1}, Siltronix, Neuchâtel, Switzerland) with a 0.5% solution of hydrofluoric acid for 20 s. (*Warning*: This operation should be executed in a well-ventilated fume hood and one should wear appropriate protection.) The resulting Si substrates had a root-mean-square roughness of 0.2 nm as measured with an atomic force microscope (AFM, see below), with advancing and receding contact angles with water (measured $\approx$ 5 min after the HF etch of the oxide layer) of 90 $\pm$ 2° and 62 $\pm$ 5°, respectively. These surfaces were used within 1 h of their preparation to minimize regrowth of a SiO_2 overlayer. Si was a particularly convenient substrate in many of our studies, providing excellent attachment of IgGs and demonstrably flat (see below) surfaces helpful for AFM. Glass slides (Menzel−Glaeser, Germany), sensor chips SiO_2/TiO_2 (ASI 1400, Balzers, Liechtenstein), and the SiO_2 surfaces of Si wafers were cleaned for 10 min with H_2SO_4:H_2O_2 (3:1) (*Warning*: This solution is a powerful oxidant and reacts violently when mixed with certain compounds) and then rinsed copiously with deionized water ($\approx$200 mL). These surfaces were subsequently aminopropylated in a 10% aqueous solution of (aminopropyl)triethoxysilane (Fluka) for 3 h at 80 °C. The pH was adjusted to $\approx$6.5 with acetic acid. The aminopropylated substrates were rinsed with deionized water and dried at 120 °C for at least 3 h before they were activated with a *N*-hydroxysuccinimide ester (NHS) on the surface (bis(sulfosuccinimidyl)suberate, BS,[3] Pierce) to promote adhesion of the IgGs by their covalent addition. The cross-linker was prepared as a 5-mM solution in sodium acetate buffer (10 mM, pH 5.0). Alternatively, self-assembly of a monolayer of an alkanethiol terminated by *N*-hydroxysuccinimide ester[15,16] on evaporated films of Au[17] formed a similarly reactive surface. Polystyrene culture dishes (Falcon Optilux 1001, Becton Dickinson, Lincoln Park, NJ) were rinsed with 2 $\times$ 10 mL of ethanol and dried under a stream of N_2 before their use.

Preparation of μFNs. Fluidic networks were formed from PDMS (Sylgard 184, Dow Corning, Midland, MI). The prepolymer components of Sylgard 184 were combined following the recommendations of the manufacturer using an automatic dispenser (DOPAG MICRO−MIX E, Cham, Switzerland). The mixture was poured directly on a master and cured at 60 °C for 24 h. These masters had a negative

(4) Kim, E.; Xia, Y.; Whitesides, G. M. *J. Am. Chem. Soc.* **1996**, *118*, 5722−5731.
(5) Delamarche, E.; Bernard, A.; Schmid, H.; Michel, B.; Biebuyck, H. A. *Science* **1997**, *276*, 779−781.
(6) *Immunoassay*; Diamandis, E. P., Christopoulos, T. K., Eds.; Academic: San Diego, CA, 1996.
(7) Fodor, S. P. A.; Read, J. L.; Pirrung, M. C.; Stryer, L.; Lu, A. T.; Solas, D. *Science* **1991**, *251*, 767−773.
(8) Rozsnyai, F.; Benson, D. R.; Fodor, S. P. A.; Schultz, P. G. *Angew. Chem., Int. Ed. Engl.* **1992**, *31*, 759−761.
(9) Bhatia, S. K.; Hickman, J. J.; Ligler, F. S. *J. Am. Chem. Soc.* **1992**, *114*, 4432−4433.
(10) Lopez, G. P.; Biebuyck, H. A.; Haerter, R.; Kumar, A.; Whitesides, G. M. *J. Am. Chem. Soc.* **1993**, *115*, 10774−10781.
(11) Southern, E. M.; Case-Green, S. C.; Elder, J. K.; Johnson, M.; Mir, K. U.; Wang, L.; Williams, J. C. *Nuc. Acids Res.* **1994**, *22*, 1368−1373.
(12) Sundberg, S. A.; Barrett, R. W.; Pirrung, M.; Lu, A. L.; Kiangsoontra, B.; Holmes, C. P. *J. Am. Chem. Soc.* **1995**, *117*, 12050−12057.
(13) Schena, M.; Shalon, D.; Davis, R. W.; Brown, P. O. *Science* **1995**, *270*, 467−470.
(14) Chee, M.; Yang, R.; Hubbell, E.; Berno, A.; Huang, X. C.; Stern, D.; Winkler, J.; Lockhart, D. J.; Morris, M. S.; Fodor, S. P. A. *Science* **1996**, *274*, 610−614.
(15) Wolf, H. Ph.D. Thesis, Institut für Organische Chemie, Johannes Gutenberg Universität, Mainz, Germany, 1995.
(16) Wagner, P.; Hegner, M.; Kernen, P.; Zaugg, F.; Semenza, G. *Biophys. J.* **1996**, *70*, 2052−2066.
(17) Delamarche, E.; Sundarababu, G.; Biebuyck, H. A.; Michel, B.; Gerber, Ch.; Sigrist, H.; Wolf, H.; Ringsdorf, H.; Xanthopoulos, N.; Mathieu, H. J. *Langmuir* **1996**, *12*, 1997−2006.

pattern of the desired μFN defined in photoresist (Hoechst 6612, 1.5 μm thick) by optical lithography and were coated everywhere with ≈10 nm of a plasma-polymerized, fluorinated layer (ASE−ICP, Surface Technology Systems, Bristol, UK). Individual μFNs were cut from the master replica on a polystyrene dish. Filling pads, defined in the network, were pierced from the backside of the network with an awl or cut transversally to open a path for incoming liquids. We used an O_2 plasma treatment of the μFN (oxygen pressure ≈0.8 Torr, load coil power ≈ 200 W, 15 s; Technics Plasma 100−E, Florence, KY) to render its surface hydrophilic prior to use. These surfaces had a useful lifetime in air, as judged by contact angles, for ≈15 min prior to their reconstruction to yield a hydrophobic interface.

Utilization of μFNs. The μFN was placed by hand onto the substrate under its own weight. Each independent set of channels was filled by placing a submicroliter drop of solution at one end of their openings. Reaction of the IgGs with the surface proceeded in the μFN for 1 h at solution concentrations of 1 mg mL^{-1} solution of IgGs in PBS, unless stated otherwise. The μFN was then quickly removed (1 s) from the substrate under a flow of PBS (≈10 mL) to effect a rapid dilution of unreacted materials and thus to prevent the IgGs from spreading into channels in adjacent zones or onto other parts of the substrate.[18] The substrate was rinsed three times with 1.5 mL of PBS, three times with 1.5 mL of 0.5% Tween 20 (Fluka) in PBS, and three times with 1.5 mL of deionized water to remove partially bound proteins and dried under a stream of N_2.

Immunoassays. Sites of adsorption that remained free after patterned derivatization of substrates using μFNs (see above) were blocked by exposing the substrates to a solution of 1% bovine serum albumin (BSA, Sigma) in PBS for 45 min at room temperature. Rinses with 3 × 1.5 mL of PBS, 3 × 1.5 mL of 0.5% Tween 20 in PBS, and 3 × 1.5 mL of deionized water followed, and the substrate was dried under a stream of N_2. The immunoassays were prepared by incubating the substrate with solutions of antispecies IgGs (≈ 100 μL cm^{-2} of surface) for 30 min, then rinsed and dried as above. Tagged antispecies IgGs (Sigma Immunochemicals) were used in 1:300 dilution in PBS and detected individually using a fluorescent microscope: polyclonal anti-chicken IgGs (developed in rabbit) tagged by tetramethyl rhodamine isothiocyanate (TRITC, red, λ_{FE} = 570 nm), anti-mouse IgGs (developed in sheep) tagged by fluorescein isothiocyanate (FITC, green, λ_{FE} = 525 nm), and anti-goat IgGs (developed in rabbit) tagged by R-phycoerythrin (red-orange, λ_{FE} = 578 nm). There were 4−5 fluorophores on average per IgG according to the supplier.

Instrumentation. Wettability by aqueous buffers of surfaces was determined with a Krüss (Hamburg, Germany) contact angle goniometer equipped with a motorized pipet (Matrix Technology, Nashua, NH). A new polypropylene tip was used for each measurement to deliver the probe liquid. Advancing and receding angles were measured at three or more locations on each sample.

Coupling of IgGs to the NHS-activated surface of a sensor chip (ASI 1400, Balzers, Liechtenstein) was followed by a grating coupler sensor (BIOS−1, Artificial Sensing Instruments, Zurich). The active region in this sensor had dimensions of 8 × 2 mm^2 and was located in the center of a semicircular cell (cross section 1.7 mm^2, volume 12 μL) aligned in the direction of the flow (10 μL min^{-1}). Refractive index changes in the vicinity of the waveguide were followed by a time and refractive index resolution of 0.1 s and 1 × 10^{-7}, respectively, interpreted using the software supplied with the instrument.[19]

Optical inspection of the samples was carried out with a Leica Polyvar SC microscope equipped with long-working-distance objectives, a charge-coupled device camera (3−CCD Donpisha, Sony), and a high-resolution (768 × 512 pixels) frame grabber. Fluorescence images were obtained using a Nikon Labophot−2 microscope equipped with narrow ($\Delta\lambda$ = 20 nm) band-pass filters, a 100-W Xe lamp, and a charge-coupled device camera cooled to 0 °C (ST−8, SBIG, Santa Barbara, CA). The images (1530 × 1020 pixels, 16 bits per pixel, 3−7 s shutter times) were captured and analyzed using a software for this camera (Skypro, Software Bisque, Golden, CO).

Visualization of Au patterns on Si was performed using a Hitachi S−4000 scanning electron microscope. The AFM was a Dimension 3000 microscope (Digital Instruments, Santa Barbara, CA) operated in air in the tapping mode with TESP silicon cantilevers (Digital Instruments, resonance frequencies ≈ 250 kHz). The cantilevers had a monolayer of dodecyltrichlorosilane (ABCR, Karlsruhe, Germany) formed by a gas-phase reaction of the vapors of this silane with its surface, previously cleaned by exposure to an air plasma for 10 min at reduced pressure (≈10 Torr). The silanization of the cantilever yielded a well-defined tip with a low surface energy. All images shown in Figure 7 were recorded with the same cantilever, within 10 μm of the same coordinates on the sample, at a scanning angle of 0°, and an acquisition speed of 1.8 Hz.

Results and Discussions

Fabrication of μFNs. PDMS offers a simple, convenient, and economical choice of material for making μFNs. It is easy to handle and polymerize and readily replicates features in a predefined master.[2,20] Not all topologies on its surface are possible, however, as we showed in a previous paper.[21] Care must be taken to avoid unsupported structures with aspect ratios greater than 1 in this polymer. Such features can collapse or have poor definition in the soft elastomer, Figure 2. This softness of PD

MS is nonetheless necessary for its application to μFNs and μCP as it allows the polymer to adhere and hold the substrate on contact, occlusively sealing the surface. The contact is reversible; however, as PDMS μFNs are easily peeled off typical substrates with only moderate force (≈1 Nm^{-1} at peel rates of 0.5 mm^{-1}) and without leaving significant residue. Other material choices for μFNs, silicon for example, might have better structural and chemical properties but cannot easily be made to seal common substrates such as glass or polystyrene. The use of solvents or concentrated reactants that swell, dissolve, or corrode PDMS obviously compromise the μFN technique, although many reactions remain possible. In particular, PDMS is inert toward aqueous solutions with pH ranging from <1 to ≈12 for times of exposure in excess of several hours, enabling the use of these elastomeric μFNs for reactions carried out under physiological conditions. An additional positive aspect of PDMS μFNs is their low cost. A 4″ silicon wafer used as a mold provides enough space for ≈50 × 1 cm^2 μFNs patterns and can be replicated many times. Individual μFNs are simply cut before use from the larger replica. PDMS μFNs thus have a high experimental value and are virtually (but not necessarily) disposable after each experiment.

Filling of the μFN. In its application to the spatial confinement of a surface chemical reaction, the μFN must be filled by a liquid carrying reactants after it contacts the substrate targeted for derivatization.[22] What are the characteristics and limits of filling micron-scale capillaries in μFNs? The laminar flow of a liquid in a capillary follows the equation[23]

$$\bar{v} = \frac{C_g}{\eta} \cdot \frac{\Delta p}{l} \qquad (1)$$

The mean speed of the liquid $\bar{v}$ is proportional to the pressure drop, Δp, driving a volume of liquid filling the channel over a length l. The factor C_g/η is a friction parameter, or dissipation term, where C_g contains the geometric boundaries of the capillary, required by the condition that the liquid velocity is

(18) Alternatively, a rinse with ethanolamine can effect a rapid quenching of residual NHS groups on the surface.

(19) Bernard, A.; Bosshard, H. R. *Eur. J. Biochem.* **1995**, *230*, 416−423.

(20) Kumar, A.; Whitesides, G. M. *Appl. Phys. Lett.* **1993**, *63*, 2002−2004.

(21) Delamarche, E.; Biebuyck, H. A.; Schmid, H.; Michel, B. *Adv. Mater.* **1997**, *9*, 741−746.

(22) Kim, E.; Whitesides, G. M. *J. Phys. Chem. B* **1997**, *101*, 855−863.

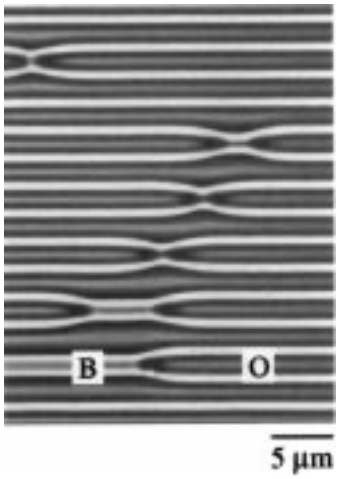

Figure 2. PDMS has only limited structural strength and is prone to deformation. This optical micrograph shows the lateral collapse and pairing of PDMS walls in a putative μFN (1.2 μm high, 0.8 μm wide) in the soft elastomer. Channels are blocked (B) or left open (O) after the stresses of forming, handling, and using the μFN.

zero at the walls, and the viscosity is η. The pressure drop is described principally by the capillary pressure for the small (<1 mm) dimensions of our μFNs

$$P_c = \gamma\left(\frac{\cos(\theta_{\text{substrate}}) + \cos(\theta_{\text{PDMS}})}{a} + \frac{2\cos(\theta_{\text{PDMS}})}{b}\right) \quad (2)$$

for a channel with a rectangular cross section of width b and height a. Its expression reveals that filling of the μFN is highly sensitive to the surface tension of the liquid, γ, and to the contact angles θ_{PDMS} and $\theta_{\text{substrate}}$ of the liquid with each of the walls of the μFN. Small channel dimensions easily lead to high values of P_c, e.g., about 10 kPa in 10-μm-sized channels when its walls are wettable ($\Theta_a < 10°$). A capillary open at only one end has $\Delta p = P_c + \Delta p_{\text{int}}$. The value of Δp_{int} is zero for capillaries open at both ends. The high solubility of such gases as N_2 and O_2[24] in PDMS also makes this term relatively unimportant for capillaries open at only one end. We routinely filled such capillaries completely even when their cross section was only 1 μm^2. We found that the velocity of the liquid was typically around 40% slower in these closed capillaries compared to their open counterparts.

Aside from its influence on the capillary pressure, the size of the μFN plays a more important role in controlling the rate of its filling via the geometric term, C_g, in determining the capillary friction. In many cases it proves sufficient to approximate this quantity by[25]

$$C_g = \frac{1}{8}\left(\frac{ab}{a+b}\right)^2 \quad (3)$$

Thus, the velocity of the liquid in a capillary is proportional to the diameter of the channel, i.e., smaller capillaries tend to fill more *slowly* than larger ones.

The time, t, the liquid takes to travel a length l in the channel is calculated by

$$t = \frac{\eta}{2\Delta p C_g} l^2 \quad (4)$$

In principle any wettable channel can be filled to its end with liquid, given enough time. Inhomogeneities, impurities, and changes in the wettability of the μFN provide the limits in real cases. The latter is particularly important for PDMS μFNs. PDMS is hydrophobic and has an advancing contact angle with water of $\Theta_{\text{adv}}^{\text{H}_2\text{O}}$. A simple plasma treatment[26] of the PDMS μFN lowers its contact angle with water to 0°,[27] allowing use of the conduits with aqueous buffers.[28] This change in the surface wettability of the polymer is not permanent, however.[29] Reconstruction of the polymer restores a hydrophobic character to its surface[30] in ≈15 min at room temperature unless the μFN contacts water.[31] In typical experiments using μFNs with channels 10 μm wide and 1.5 μm deep and polystyrene as a substrate ($\Theta_{\text{adv}}^{\text{PBS}} = 110°$), we measured that PBS buffer filled 10-mm-long, open channels in ≈8 s, in agreement with the calculated time [eq 4] assuming $\gamma = 70$ mN M^{-1}, $\eta = 1.2$ mPa and with $\Delta p = 40$ kPa and $C_g = 1.7 \times 10^{-13}$ m^2. Thus changes in the properties of the μFN during filling could be neglected. We also used unmodified PDMS blocked by BSA in some cases to make the surface wettable and resistive to passive adsorption of proteins.

Immobilization of Immunoglobulins on a Surface Using a μFN. Next, having established how to fill a μFN with buffer, we attempted to use them to direct protein coupling on a silica surface. We first characterized our prototypical immunocomplexation reaction using a waveguide sensor, Figure 3, to establish the success of the chemistry and the avidity of the antibody system. The aminopropylated surface of the sensor chip was activated with a BS^3 cross-linker[32] capable of irreversibly attaching immunoglobulins by forming amide bonds with the protein.[33] Recognition of the immobilized chicken IgGs proved specific for anti-chicken IgGs tagged with a TRITC fluorophore and demonstrated the basic characteristic of the

(23) The flow of liquid in the capillaries of the μFN is laminar because it is characterized by a small Reynolds number (Re < 1). Pressure and viscosity dominate in this regime, whereas inertial forces can be neglected.

(24) *Silicon-Based Polymer Science*; Zeigler, J. M., Gordon Fearon, F. W., Eds.; Advances in Chemistry Series, American Chemical Society: Washington, 1990.

(25) This approximation contains the so-called hydraulic radius $R_h = ab/(a+b)$ defined, in general, as the ratio of twice the cross-sectional area to the circumference of the capillary, where a and b in this equation are its width and height. Solving, in detail, the Navier−Stokes equation for rectangular-shaped channels yields a more accurate solution (see: Spurk, J. H. *Strömungslehre*; Springer: Berlin, 1996):

$$C_g = \frac{a^2}{4}\left(\frac{1}{3} - \frac{a}{b}\frac{64}{\pi^5}\sum_{n=1}^{\infty}\frac{\tanh((n-1/2)\pi b/c)}{(2n-1)^5}\right)$$

The summation can be reduced to its first and second components to facilitate calculation. We find that for aspect ratios in the range $0.25 < a/b < 4$ the error in the hydraulic radius approximation is <13%.

(26) Wet oxidation of PDMS using acids is also possible (Ferguson, G. S.; Chaudhury, M. K.; Biebuyck, H. A.; Whitesides, G. M. *Macromolecules* **1993**, *26*, 5870−5875). When the μFN was used on a hydrophilic surface, such as treated glass or carboxylic acid-terminated monolayers, coating the μFN walls with BSA proteins (by 1-h equilibration of a 1% BSA solution in PBS on the μFNs) appeared sufficient to provide good filling. In another case, adding ethanol to the aqueous buffer (up to 5% in volume) allowed the μFNs to be filled even when their geometry proved unfavorable.

(27) Chaudhury, M. K.; Whitesides, G. M. *Langmuir* **1991**, *7*, 1013−1025.

(28) Organic solvents, or solutions with detergents, typically have a much lower surface tension and are more able to wet PDMS, proving less problematic as regards filling.

(29) Extended times of exposure to O_2 plasma treatments do not prolong the lifetime of the wettable surface in air. Shorter treatments, or treatments with lower plasma powers, yielded equally hydrophilic μFNs but possibly with less wetting homogeneity of the resultant micron-sized capillaries.

(30) For a general description of this phenomenon, see: Holmes-Farley, S. R.; Reamey, R. H.; McCarthy, T. J.; Deutch, J.; Whitesides, G. M. *Langmuir* **1984**, *1*, 725−740.

(31) Once plasma-treated, μFNs in air were filled with liquid within ≈10 min to minimize their loss of wettability by reconstruction of the polymer surface or its contamination from the ambient. Storage of freshly activated μFNs in deionized water proved useful in maintaining their hydrophilicity for long times (>100 h).

methodology used throughout the rest of the paper: (1) an antigen is fixed on a surface and (2) the antigen is detected by the specific binding of its antibody partner from a solution wetting the entire substrate. Step 2 is obviously sensitive to the type, condition, and orientation of the immobilized antigen, but we generally found that more than 60% of the surface species were recognized by polyclonal antibodies.

Depletion of Reactants within a μFN. One important difference between the deposition of proteins in the cell of our grating coupler and their reaction in the channels of a μFN is that the driving force for flow in the latter exists only until the network is filled. Again we wanted to rely exclusively on hydrodynamic forces to supply the μFN so as to maintain the greatest possible simplicity in our approach. Thus only a limited amount of reactants was available in the conduits so that their loss onto the substrate and the walls of the conduits strongly affected the local probability of reaction at different points of the network.

A second important difference between reactions in the cell of our sensor and those of a typical μFN is the degree of the divergence between the nominal concentration of reactants in solution and that of molecules available for attachment at the surface. Diffusion effects are exacerbated in the larger volume of the sensor where the boundary layer is much thicker (we estimate at least 100 μm). Diffusion of molecules to the walls of a μFN occurs very quickly (within milliseconds, see below) by contrast. Mass transport limitations to surface chemical reactions are therefore less important in μFNs, and the time scale of reactions there can be much smaller than found even in the already small volumes of our waveguide sensors (see Experimental Section). Depletion of reactants in μFNs is then principally controlled by their surface-to-volume ratio and not the boundary-layer thickness.

Figure 4 provides a striking example of effects of depletion in a μFN. Here, we examined a network opened at only one end. Such "closed" networks could be useful, in principle, to minimize contamination between the flows in adjacent channels and over other parts of the substrate as fluid exits the network. A reaction, as observed by the resulting pattern of fluorescence, evidently occurred only over a very limited distance from the opening of the network, although the liquid solution filled the *entire* length of the conduits (see above). This observation was independent of the time of coupling to the surface. Changing the conditions of plasma activation of the μFN or the pH of the solution similarly had no effect on improving the scale of derivatization, suggesting that electrostatic repulsion between the walls of the μFN and the charged proteins was not responsible for limiting the spatial extent of reaction. The concentration of protein in the solutions that filled the μFN had the expected influence on the scale over which derivatization occurred, although the distance always remained <100 μm in closed networks for concentrations of protein up to 1 mg mL^{-1}, already much higher than is practical. These data suggest that the solution was increasingly depleted of reactants as it traveled along the conduits of the μFN. Depletion of reactants in closed networks is a general problem caused by the absence of continuous flow. Figure 4D is an example of this phenomenon with a very different chemical reaction: It shows a millimolar solution of an alkanethiol forming a monolayer on a gold substrate.[34] The solution filled the length of a 3-mm-long set of closed capillaries. Adsorption of the thiol to form a monolayer capable of withstanding an etch-based assay of its presence[35] again occurred over $<5\%$ of the length of the conduits.

How can we understand the results in Figure 4? When a solution fills a channel, its velocity is greatest at the beginning of the capillary and diminishes toward the end. The profile of its flow has a velocity maximum in the center of the channel and drops to zero at the walls. Motion of reactants in the solution is then a superposition of their diffusion and the local flow. Thus diffusion largely governs the flux of proteins, or other molecules, to the surface. Although the diffusion constant of proteins is small, typically $D \approx 10^{-7}$ cm^2 s^{-1}, its effects are dramatic at the micron scale.[36] Simulations[37] show that when particles with the diffusion constant of a protein enter a channel having micron-scale dimensions, 95% of them collide with one of its walls within $\approx$15 ms, corresponding to a distance of travel along the network of no more than 100 μm. If the interaction between the two is sufficiently strong, the protein is effectively removed from solution. This leads to deposition from the beginning of the channel—or more precisely from the beginning of the pad—until the solution is depleted or the walls are covered with protein. Neglecting the short transition region in surface coverage evident in Figure 4, the length of deposition is related to the amount of proteins passing through the channel, given by the concentration and volume of its solution, that transfers into a surface coverage of the substrate and walls. We calculate[38] that wettable capillaries having a 10×1.5 μm^2 cross section and a length of 3 mm require a minimum of twice their volume simply to ensure sufficient reactants for the surface area under our typical conditions. This excess volume is even greater in real situations where depletion of reactants already starts in the filling pads.[39] To achieve a long-range deposition in a μFN for a given geometry (i.e., the surface-to-volume ratio) and

(32) The density of NHS termini on the surface available for binding was difficult to estimate because of the topography of the substrate, the degree of aminopropylation of the chip, and the possibility of unproductive reactions of BS^3 and the surface. The change measured by ellipsometry in surface coverage after reaction with BS^3 on the surface was $\approx$1 ng mm^{-2} ($a \approx$ 1-nm-thick layer) and suggested an occupancy of $\approx$4 NHS nm^{-2}. We have not established the details of the reaction between this surface and proteins other than to satisfy ourselves that their coupling appeared covalent, maintaining protein-associated mass on the surface even under highly denaturing conditions such as rinses with organic solvent.

(33) Hermanson, G. T.; Mallia, A. K.; Smith. P. K. *Immobilized Affinity Ligand Techniques*; Academic: London, 1992.

(34) Bain, C. D.; Troughton, E. B.; Tao, Y.-T.; Evall, J.; Whitesides, G. M.; Nuzzo, R. G. *J. Am. Chem. Soc.* **1989**, *111*, 321−335.

(35) Kumar, A.; Biebuyck, H. A.; Abbott, N. L.; Whitesides, G. M. *J. Am. Chem. Soc.* **1992**, *114*, 9188−9189.

(36) For an IgG, $D \approx 4 \times 10^{-7}$ cm^2 s^{-1}, see: Sjölander, S.; Urbaniczky, C. *Anal. Chem.* **1991**, *63*, 2338−2345.

(37) We approximated the 2D diffusion equation

$$\frac{\partial c}{\partial t} = D\left(\frac{\partial^2 c}{\partial x^2} + \frac{\partial^2 c}{\partial y^2}\right)$$

by a superposition of the 1D analytical solutions for a conduit with dimensions 1.5×10 μm^2, corresponding to the cross section of the channel. We used $D = 4 \times 10^{-7}$ cm^2 s^{-1} and started with a constant concentration distribution. The concentration of proteins at the boundaries was kept at 0 (i.e., proteins were removed from the simulation on touching a wall).

(38) We estimated the length of deposition $d \approx abc/(b\tilde{c}_{\text{substrate}} + (2a + b)\tilde{c}_{\text{PDMS}} + abc)\cdot l$, where a and b are the height and the width of a channel filled to a length l, the concentration in the liquid is c, and $\tilde{c}_{\text{substrate}}$ and $\tilde{c}_{\text{PDMS}}$ are the final surface coverages on the substrate and PDMS. Using a channel closed at one end (10×1.5 μm^2) and a protein concentration of 1 mg mL^{-1}, protein deposition is expected only on the first half of its length, assuming a surface coverage of $\approx$1 ng mm^{-2} and a high interaction probability between the proteins and the walls. We note that this model, which accounts for our observations of depletion in μFNs, involves only surface deposition phenomena (i.e., proteins do not diffuse into the bulk elastomer).

(39) A block of the walls of the μFN with BSA to prevent passive deposition also alleviated depletion and provided the network with a reasonable wettability, sufficient to achieve good filling on some—but not all—substrates.

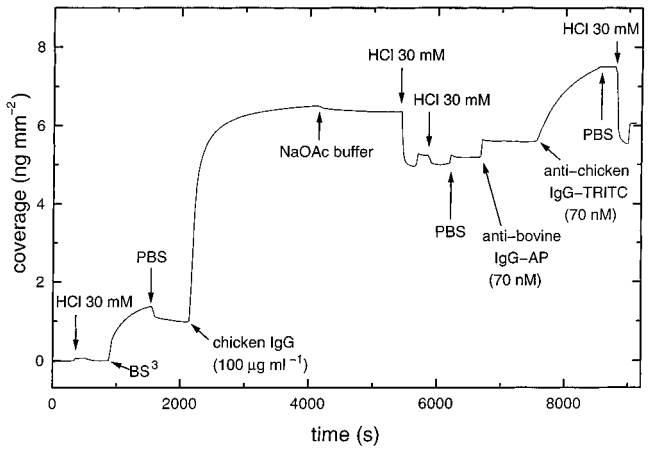

Figure 3. Characterization of the preparation and outcome of an immunocoupling reaction on the glass surface of a buried waveguide sensor. This figure plots the temporal coverage of the active sensor region calculated from changes in the effective refractive index of its surface and the nearby (<100 nm) solution environment. The surface was first activated by an aminopropylation reaction (not shown). Recognition of the immobilized chicken IgGs occurred specifically (anti-chicken IgG) with no detectable nonspecific response (anti-bovine IgG). The latter IgGs were tested with (shown) and without (not shown) tags (TRITC and alkaline phosphatase) to simulate more closely the conditions of coupling in our μFNs.

solution concentration, therefore, the flow must be sufficiently large to provide enough reactants to the targeted area.

Design and Use of μFNs. The outcome of the previous sections suggests some guidelines for the implementation of useful μFNs. A flow-promoting pad connected to the end of the array of channels, Figure 5, is needed to effect the renewal of reactants through the network. This pad supplies an outlet for liquid from the μFN outside of the areas on the substrate targeted for reaction and maintains a similar capillary force [$P_c \approx 40$ kPa, $b \rightarrow \infty$, eq 2] on the system. The liquid content of 100 channels, each having a volume of 13 pL (the volume of a 3-mm-long channel with a cross section of 3×1.5 μm^2), exchanged ≈10 times by the addition of a 15 nL flow-promoting pad (a 1.5-μm-thick pad with a surface of 10 mm^2 was typical in our experiments). This small volume emphasizes the maintenance of the overall economy of reactants with μFNs.[40] The incorporation of posts (25 μm^2) regularly spaced inside the pads contributed to the stability of the large, but thin, cavities by preventing their collapse and adventitious contact with the substrate. Figure 5 shows an example of such a μFN that successfully delivered reactants along the entire length (3 mm) of its 3-μm-wide channels.

Figure 6 shows that no evident depletion of chicken IgGs occurred along the channels in a μFN formed as described above and used under the same coupling conditions as in Figure 4. Detection of the immobilized IgGs by their binding to anti-chicken IgGs applied to the patterned substrate from a bulk solution indicated, in addition, the preservation of a useful percentage of the binding properties of these immobilized proteins.[41] The level of fluorescence emitted by tagged secondary IgGs specifically coupled to IgGs on the surface of either pads and in all the channels contrasts with the dark background in adjacent zones of the substrate covered by PDMS in the μFNs during patterning. The emitted light levels in these areas were between 5 and 10 times that of the background depending on

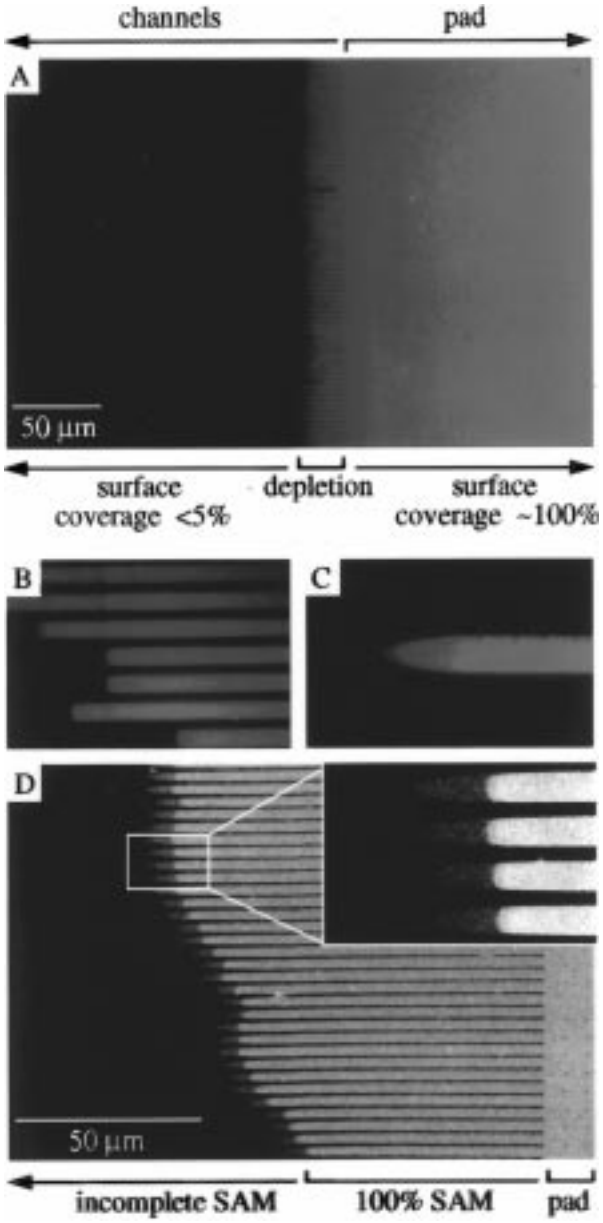

Figure 4. Depletion of reactants delivered by a μFN to a surface occurs by their loss onto the walls of the channels or by reaction with the substrate and is very sensitive to the flow of fluid through the network. (A) The fluorescence image shows the result of immunocomplexation of chicken IgGs patterned by a μFN onto NHS-activated glass by TRITC-anti-chicken IgGs delivered from solution. The μFN used here had closed channels 1.5 μm deep, 3 μm wide, and 3 mm long that filled *completely* during the experiment but did not allow flow through the network. Derivatization of the surface was consequently seen only near (<100 μm) the openings of the macroscopic filling pads. Patterns of depletion in 10-μm-wide capillaries on hydrophobic silicon showed plug (B) or tapered profiles (C) depending on whether filling was intermittent or continuous, respectively. Depletion-related phenomena using μFNs were similarly observed for other reactions (D) such as the chemisorption of hexadecanethiol on Au from 1 mM solution in ethanol. Here a cyanide-based etch of underivatized Au was the diagnostic for the presence of self-assembled monolayers (SAMs): Light regions in the scanning electron microscopy image are SAM-protected gold; dark regions are the silicon wafer where the unprotected gold had been etched away.

the substrate and its characteristics and had signal-to-noise ratios of ≈70 per 0.25 μm^2 for integration times of 7 s with our camera. This result suggests that sealing of the channels

(40) Our typical experiment consumed ≈ 1 μL because of the additional volume associated with the entrance into the filling pad, which was a hole pierced through the elastomer from the backside of the μFN.

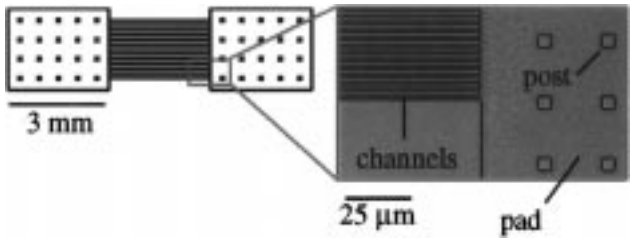

Figure 5. Scheme illustrating how to facilitate flow through a μFN where only capillary forces act. One pad supplies liquid and reactants while the other opens the channels and draws liquid through the network. Square posts, regularly spaced in the pads, prevent their collapse on the surface. The inset at the right is an optical photograph of part of a PDMS μFN having 3-μm-wide, 1.5-μm-deep channels separated by $\approx$1 μm.

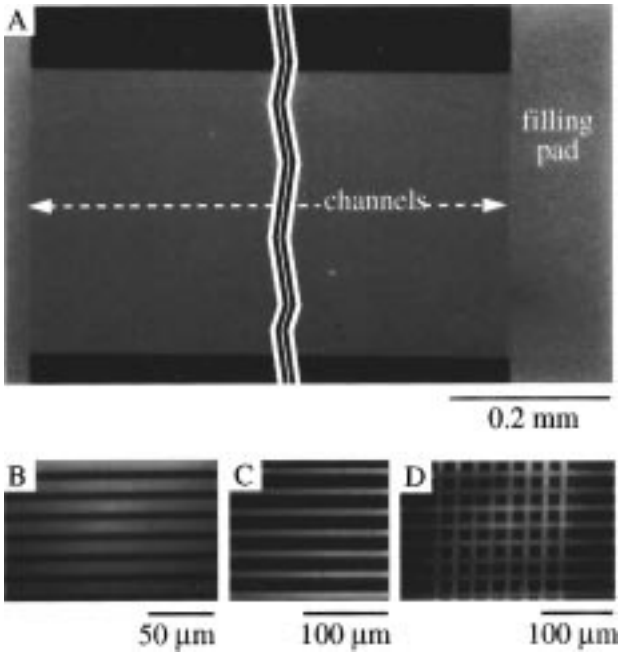

Figure 6. Allowing flow through a μFN caused homogeneous derivatization of different substrates over the entire length (3 mm) of the network. These representative fluorescence images indicate that delivery of chicken IgGs with μFNs, and detection by anti-chicken TRITC−IgGs from solution, was largely faithful to the dimensions of the μFN on scales from microns to millimeters. Channels were 1.5 μm deep in all cases. Immobilization of the primary IgGs occurred inside (A) 3-μm-wide channels on NHS-activated glass, (B) 10-μm-wide channels on hydrophobic Si, or (C, D) on polystyrene. In the latter image, the pattern is formed by consecutive use of two μFNs with identical geometry on the same polystyrene substrate. All immobilization reactions were carried out under similar conditions in these experiments, carried out for 1 h in the μFN prior to its release.

remained relatively effective (see below, however) during the 1-h duration of reaction. Similarly, release of the μFN under a flow of PBS buffer did not appear to compromise the contrast in protein location by contamination of untreated parts of the substrate. Analysis of the fluorescence distribution within these lines showed that the signal outside of the geometric flow boundaries decayed to background $\approx$5 μm from the edge of the targeted area. This result suggested a small leakage or diffusion of proteins under the PDMS at scales of 5 μm (see below).

One of the principal advantages of the μFN technique lies in its ability to pattern many different types of substrates because of the general quality of the seal of a substrate by its conformal contact with PDMS. This fact makes μFNs attractive for use with hydrophobic substrates where monolayer quantities of proteins adsorb nonspecifically: Silicon (with its oxide removed) and polystyrene are examples of this type of surface that were also successfully patterned with 10-μm-wide lines of proteins using μFNs, shown in Figure 6 (parts B and C, respectively). Successive use of μFNs on the same substrate to form more complicated patterns was also possible, Figure 6D, although with the expected amplification in the possibilities of error. The latter is attractive in cases where all steps in the immunoassay require, or benefit from, economy.

Atomic Force Microscopy of Patterns of IgGs Formed with a μFN. We used an AFM to characterize patterns of IgGs formed with μFNs because this technique images areas down to single IgGs adsorbed onto a surface and is thus the ultimate diagnostic for the placement of proteins. HF-stripped Si was used here because it offered a very flat surface[42] that facilitated the distinction of proteins and substrate and promoted the irreversible deposition of proteins, at least in part because it is hydrophobic.

The AFM images in Figure 7A show a pattern of adsorbates resulting from the use of μFN, comparable to the one in Figure 5 but with smaller channels, to place chicken IgGs onto 2-μm lines on a Si substrate. The texture of the deposited layer consists of individual IgGs (see below) with lateral dimensions in the image of 20−25 nm and heights of 2.5−3.5 nm.[43] The average thickness of the IgG layer measured by the AFM and the density of protein coverage in the zones of their deposition, estimated here to be >70%, was comparable to the thickness measured over 1-mm^2 areas by ellipsometry for a layer of chicken IgGs deposited from solution on hydrophobic silicon and other types of substrates. Si substrates covered by similar μFNs and having only PBS buffer in its channels proved indistinguishable from bare hydrophobic Si (data not shown), indicating that the PDMS elastomer and the general handling and rinsing steps did not release material detectable by the AFM onto the substrate. The edge resolution of the IgG pattern appears good in these images: The transition between zones of the surface exposed to the channels and their separating lines occurs in $\approx$100 nm. A small quantity of IgGs (corresponding to < 4% of a monolayer) is evident outside the zones of derivatization, however. The presence of these proteins was not due to contamination of the entire substrate following its release from the μFN but arose as a result of the migration of IgGs underneath the PDMS seal. Shorter times of reaction in the μFN caused a proportional loss in the coverage by IgG in the channels and similarly reduced the amount of protein present in the lines separating the channels. The degree of purity of the protein solution used with the μFN had a strong influence on the appearance of proteins in the gaps: Simple dialysis

(41) Quantization of the amount of primary IgG on the surface was possible by comparing the fluorescence signal following immunocomplexation of tagged antispecies antibodies on large (>5 mm^2) areas of a substrate and cross-correlating the results with those obtained by another technique like ellipsometry. In general, we found reasonable levels of agreement (variation < 10% for Si substrates, for example) between the surface coverages obtained using deposition from appropriately designed μFNs or bulk solution.

(42) HF-stripped wafers of silicon had a root-mean-square roughness of 0.2 nm over areas of 1 μm^2 in our experiments.

(43) These dimensions are a convolution between the "real" size of the IgG, the geometry of the tip, and its chemistry. The features nevertheless appear to be reasonable approximates of the physical situation. The purity of the IgGs used to prepare the solution for deposition strongly influenced the diversity and size of objects deposited on the surface and observed with the AFM. Filtration and dialysis of the IgG solutions using a cutoff filter of 35 kD gave the deposited proteins a reproducible and homogeneous appearance.

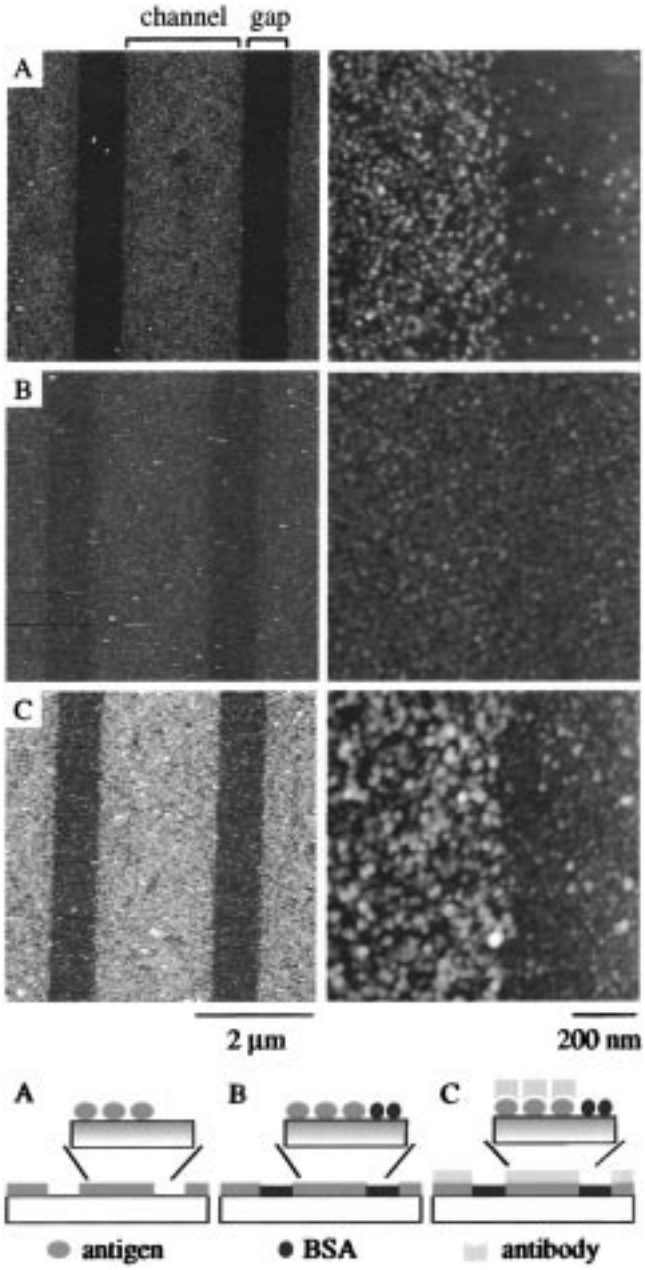

Figure 7. Patterned coverage of a surface with protein was largely complete in regions opened to the μFN with a small but significant amount of leakage outside these areas. AFM images obtained in air of (A) the patterned delivery of chicken IgGs with a μFN (as in Figure 5) onto the hydrophobic surface of a Si wafer, (B) a subsequent block of this surface by BSA to passivate "free" sites of adsorption, and (C) the immunocomplexation of immobilized IgGs by anti-chicken IgGs from solution. These images reveal the high degree of surface coverage (>70% of a monolayer) in regions opened to the μFN, and a small but significant (≈4% of a monolayer) deposition outside these areas (see text). All images in this figure were acquired on the same region (±10 μm) of the sample and are representative of all our experiments performed with the same IgG−substrate coupling conditions.

greatly minimized, but did not eliminate, the occurrence of protein in these regions, presumably by eliminating a low-molecular-weight fraction that had an enhanced diffusive mobility under the PDMS barriers from the solution. The hydrophilicity of PDMS and its microtexture could account for these observations. Selective oxidation of the μFN seems to provide a solution to this problem, although we have not explored this case systematically in the current study. We generally found that migration under the PDMS seal was

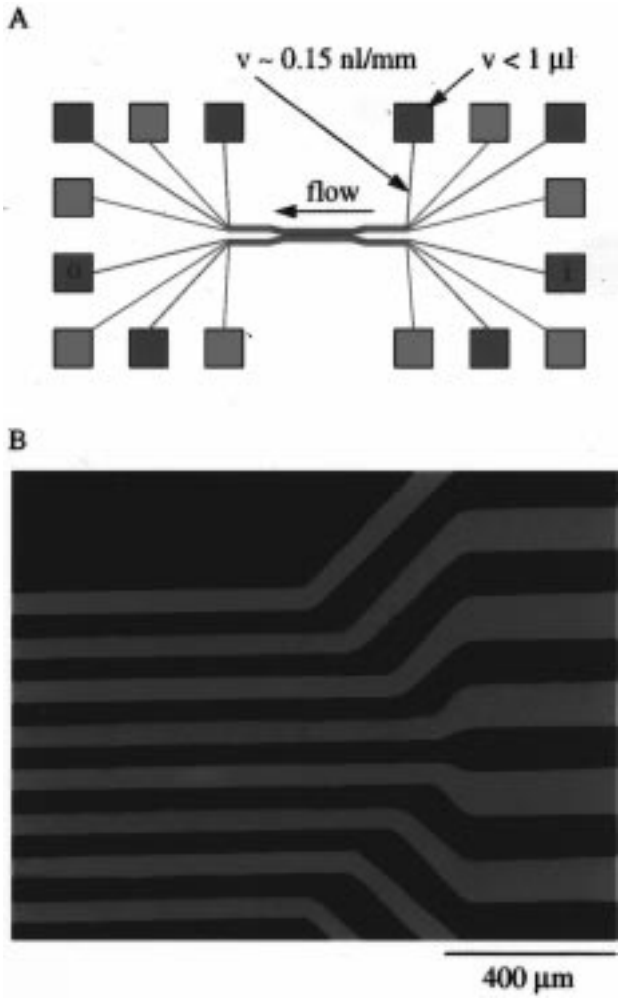

Figure 8. Simultaneous and highly localized immunoassays for the immobilized specific detection of different IgGs. (A) Scheme of the design of a μFN for the simultaneous delivery of different reactants from distant, macroscopic pads to a central zone of detection (see also Figure 1B). (B) Immobilization of chicken IgGs and monoclonal mouse IgGs on NHS-activated glass in alternative 50-μm-wide channels of such a μFN, followed by a BSA block on the entire surface, and the detection of these immobilized IgGs by exposure of the entire substrate to a solution of antispecies IgGs: anti-chicken IgGs tagged with TRITC (red, $\lambda_{FE} = 570$ nm), anti-mouse IgGs tagged with fluorescein (green, $\lambda_{FE} = 525$ nm), and anti-goat IgGs tagged with R-phycoerythrin (red-orange, $\lambda_{FE} = 578$ nm). The fluorescent image, a digital composite of intensity maps at the three possible wavelengths, shows a specific recognition on the surface. No anti-goat IgGs (<0.1% of a monolayer) were detected on the surface, indicating that the blocking step with BSA was effective in preventing nonspecific deposition of protein. Similarly, red labels were not detected in adjacent green lines and vice versa.

confined to within 5 μm of the border for 1-h reaction times, i.e., the substrate appeared indistinguishable from one not exposed to proteins in an area >5 μm from the targeted regions. This observation demonstrates the practical limit of μFN-based reactions under our experimental conditions, a limit that is not restrictive for practical applications. Modifying the conditions of the reaction, such as its time or temperature, or changing its characteristics to achieve faster coupling[17] may be equally useful.

BSA blocking of sites left free during the adsorption of the chicken IgGs is crucial for an assay based on detection of immobilized IgGs by preventing nonspecific adsorption of secondary, or recognition, antibodies. BSA is a slightly smaller

protein[44] than a chicken immunoglobulin and raised the overall protein coverage to ≈100% of the surface accessible to proteins (Figure 7B). A loss in topological contrast in the AFM-detected pattern occurred for this reason after the BSA block. This contrast was restored in part by a subsequent, and demonstrably specific, recognition of the immobilized IgGs by polyclonal anti-chicken TRITC−IgGs (having a nanomolar surface avidity for the bound antibodies) assembled onto their counterparts from a bulk solution. An overlayer of anti-chicken IgGs (≈2.5−4 nm thick) built up principally on zones covered initially by chicken IgGs. The coverage of the secondary IgG molecules appeared less homogeneous than that observed for the primary IgGs but was nevertheless surprisingly high, at least 60% (by direct count in the AFM images) that of the primary IgGs. The effects of structure, orientation, and steric hindrance on the recognition of the fixed antibodies were evidently not too compromising to immunocomplexation on these surfaces. This result is undoubtedly due, at least in part, to the use of polyclonal antibodies in the recognition step, with the expected diminution of the epitopic requirement. Figure 7C also suggests the presence of a small number of secondary IgGs in areas of the substrate not directly exposed to reactants outside the channels, like in Figure 7A, that followed the same spatial distribution as the primary immunoglobin.

Concluding Remarks: Simultaneous Assays in Small Areas

One of our motivations in using μFNs to pattern biomolecules was to allow novel assay formats and the direct incorporation of proteins on a variety of technological substrates with the possibility of their simultaneous and economical attachment. We think this report shows useful progress toward these goals. Figure 8 provides an example where a μFN creates eight isolated reaction zones in a space less than 800 μm wide. The spacing between the pads at each extremity in the channel maintained their independence and minimized contamination of material during the loading and filling of the pads. Similarly, the size of the channels and their spacing helped improve the contrast of the pattern as observed by the tagged immunoassay: The experimental conditions for this assay were equivalent to those used to detect one type of IgG fixed from solution onto substrates such as polystyrene, indicating that no new step or procedure was necessary to accomplish the fluorescent assay after construction of the pattern.

Checking for the presence, and titrating the amount, of protein fixed with a μFN on a surface using enzyme-linked types of assays is not obviously possible without another μFN to confine the enzymatic products. We think that the use of μFNs in combination with immunoassays nevertheless remains valuable and general, as it satisfies some of the sought qualities in future assay development and control. Many variants and combinations of tags and spatial patterning are clearly suitable to increase the information density. No obvious technical limitation prevents the application of μFNs to more elaborate immunoassays involving sandwich or capture types of assays, for example. High signal-to-noise analyses of these assays could result from the simultaneous use of a large number of fluorescent zones, each handled at once under identical conditions. The compatibility of μFNs with a variety of substrates should also prove useful when functional molecules are to be integrated directly onto, or into, electronic devices. In total, the use of μFNs to form patterns on surfaces has found one striking application and definitely remains open to other types of reactions and investigations.

Acknowledgment. A. Bernard is supported by a Swiss National Science Foundation NFP36 project. A. Bietsch acknowledges financial assistance through the Swiss Federal Office of Education and Science within the ESPRIT basic research project NANOWIRES (23238) and support from O. Marti (University of Ulm). We thank H. Rothuizen for his help in the design of the μFNs as well as P. Guéret (IBM Zurich) and H. R. Bosshard (University of Zurich) for their continuous support.

JA973071F

(44) BSA is described as a $4 \times 4 \times 14$ nm^3 protein composed of three domains that are differently charged but nearly equivalent in size. Peters, T. *Adv. Protein Chem.* **1985**, *37*, 161−245.